Magnetotransport studies and mechanism of Ho- and Y-doped $La_{0.7}Ca_{0.3}MnO_3$

V. Ravindranath,[1,2] M. S. Ramachandra Rao,[1,2,*] G. Rangarajan,[2] Yafeng Lu,[3] J. Klein,[3] R. Klingeler,[3] S. Uhlenbruck,[3] B. Büchner,[3] and R. Gross[3]

[1]*Material Science Research Centre, Indian Institute of Technology, Madras, Chennai 600 036, India*

[2]*Department of Physics, Indian Institute of Technology, Madras, Chennai 600 036, India*

[3]*II. Physikalisches Institut, Universität zu Köln, Zülpicher, strasse 77, D-50937 Köln, Germany*

(Received 17 May 2000; revised manuscript received 22 December 2000; published 24 April 2001)

Transport properties of mixed-valence manganites of the type $(La_{0.7-x}R_x)Ca_{0.3}MnO_3$ where $R=$Ho (magnetic) and Y (nonmagnetic) have been investigated above the ferromagnetic transition temperature (T_C). It is interesting to see that the Ho-doped compounds have less resistivity compared to the Y-doped compounds, although Ho and Y ions have almost the same ionic radii and hence lattice strain effect would be the same in both the cases. The internal magnetic field of Ho ($\mu_{eff}^{Ho}=10.5\mu_B$) is found to be responsible for this decrease in resistivity in Ho-doped compounds. Coupling of Ho magnetic moment to that of Mn has been confirmed by magnetization measurements. The resistivity data above T_C fit well to the magnetic localization model proposed by Viret *et al.* [Phys. Rev. B **55**, 8067 (1997); Phys. Rev. Lett. **75**, 3910 (1995)] and the localization lengths thus obtained are reasonable. The localization lengths of the Ho-doped compounds are greater than that of Y-doped compounds of the same composition indicating that the coupling of the Ho moment with that of the Mn moments is responsible for this effect.

DOI: 10.1103/PhysRevB.63.184434 PACS number(s): 75.30.Cr, 72.15.Gd, 71.30.+h, 75.60.Ej

Hole-doped manganese perovskites of the type $La_{1-x}Ca_xMnO_3$ (Refs. 1 and 2) exhibit colossal magnetoresistance behavior near the ferromagnetic transition temperature T_C.[3–5] This remarkable phenomenon is attributed to the magnetic coupling between Mn^{3+} and Mn^{4+} ions described as Zener's double exchange as well as to the strong electron-phonon coupling arising from the Jahn-Teller splitting of Mn $3d$ levels.[6–9] The principal factors that affect the T_C and magnetoresistance (MR) and the underlying physical mechanisms, especially in the Mott-insulator regime are still open to discussion.[10–20] It has also been observed that the Mn^{3+} -O- Mn^{4+} bond angle and the bond lengths play an important role in controlling the magnetotransport properties of the manganites as the geometric quantity, the tolerance factor *t*, is modified when smaller ions are substituted for La to fill the three-dimensional network of MnO_6 octahedra.[21] Several discrepancies with regard to T_C and MR have been attributed to grain-boundary effects, lattice strain, oxygen deficiency, etc.[22] Substitution of La by other rare earths results in the shift of the resistivity maxima ρ_m to lower temperatures due to internal pressure as the transfer interaction between Mn ions is altered.

In the present work, we have attempted to study the magnetotransport properties of $La_{0.7}Ca_{0.3}MnO_3$ (LCMO) type of compounds by replacing La with two elements (Ho and Y) of nearly the same ionic radii, however, the difference being that Ho is magnetic ($\mu_{eff}=10.4\mu_B$) and Y is nonmagnetic. The nearly equal ionic radii ($Y_{i.r}=1.018$ Å; $Ho_{i.r}=1.015$ Å) of the two substituted elements negate the effect of internal strain[22] (as the tolerance factor *t* is the same for both the cases) on the observed magnetic and electric properties. The most interesting feature of this study is that the resistivity of the Ho compounds is lesser than that of the Y compounds for identical compositions. Moreover, magnetization measurements show an increase in the saturation magnetization of the Ho-doped compounds compared to the Y-doped compounds indicating an increase in the net magnetic moment of the Mn ion and thus a probable coupling of the Ho moment to the Mn moment in the lattice. It has also been shown quantitatively here in terms of the reduction in the tilt angle between the Mn ions that the magnetic moment of the Ho ion reduces the resistivity and increases the magnetization in these compounds.

Polycrystalline samples of $(La_{0.7-x}R_x)Ca_{0.3}MnO_3$ where $R=$Ho and Y and $x=0.05$, 0.075, and 0.1 were prepared by the solid-state reaction method, which involved heating stoichiometric quantities of high pure La_2O_3, $CaCO_3$, and MnO_2 at 980 °C and 1200 °C in air, followed by intermittent grindings for 24 h. The compounds were pressed in to bar-shaped ($1\times1\times8$ mm^3) pellets and were sintered at 1500 °C for 24 h. Phase purity of the samples were ascertained by energy-dispersive analysis by x rays (EDAX) and powder X-ray diffraction. Resistivity ρ was measured using the standard linear four-probe method from 300 K down to 20 K at magnetic fields of 0 T, 4 T and 8 T. Magnetization measurements were performed using a Foner magnetometer for $4.2<T<300$ K in applied fields up to 14 T.

Powder x-ray diffractograms of the compounds, obtained using Cu-K_α radiations show single phase formation and are as shown in Fig. 1. In all cases the data fitted well to a pseudocubic structure with the lattice parameter *a* varying from 7.72 Å to 7.69 Å as *x* increases from 0.05 to 0.1. EDAX also revealed excellent homogeneity of the samples and is in good agreement with the nominal starting compositions. For example, the composition as obtained from the EDAX results for a nominal composition of $La_{0.65}Y_{0.05}Ca_{0.3}MnO_3$ is $La_{0.65}Y_{0.06}Ca_{0.3}Mn_{0.98}O_3$.

A comparison of the resistivities of the Ho- and Y-doped compounds at different magnetic fields is shown in Fig. 2. Two batches of the same compounds were synthesized at the same sintering temperature (1500 °C) and the resistivity ρ values seem reproducible up to 2–3 % of the value. The

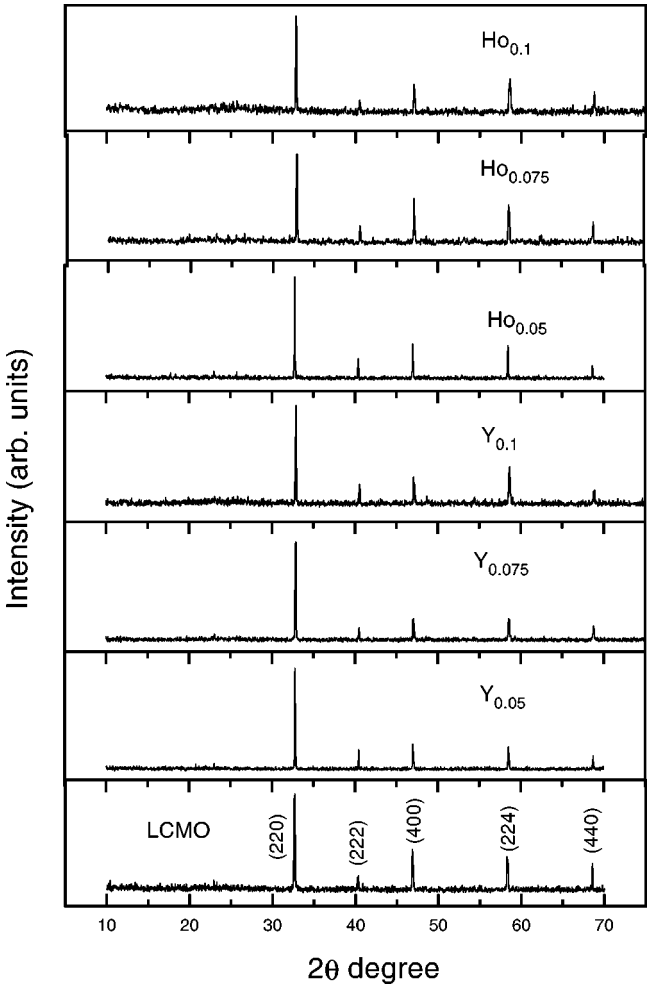

FIG. 1. X-ray diffraction plots of $(La_{0.7-x}R_x)Ca_{0.3}MnO_3$ (R = Ho, Y) with $x = 0.05$, 0.075, and 0.1 that could be indexed to a pseudocubic structure with lattice parameter a varying from 7.72 Å for $x = 0.05$ to 7.69 Å for $x = 0.1$.

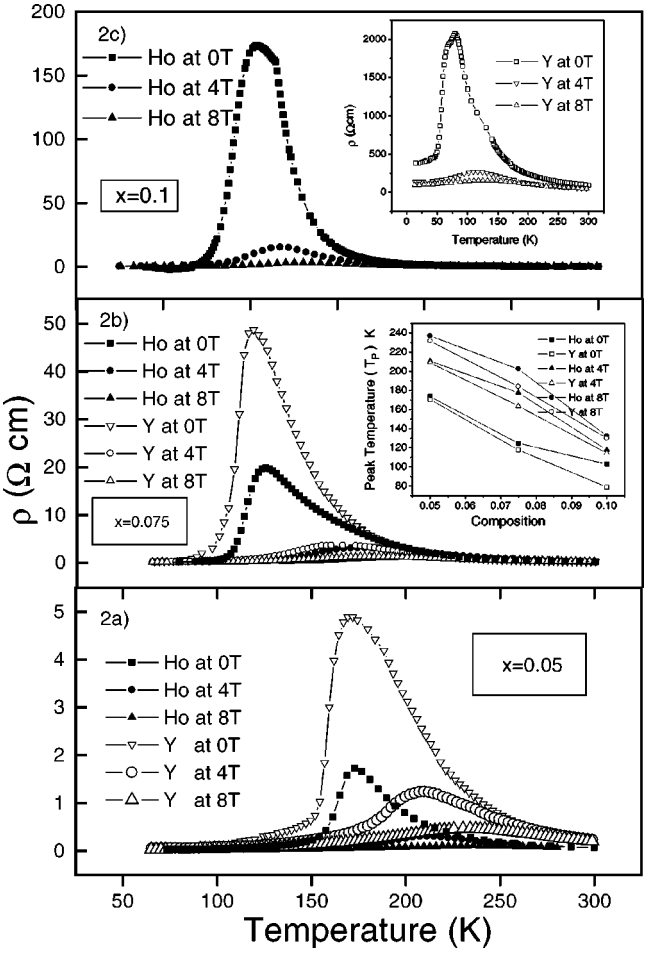

FIG. 2. Resistivity versus temperature plots at magnetic fields of 0, 4 T, and 8 T for $(La_{0.7-x}R_x)Ca_{0.3}MnO_3$ (R = Ho, Y) with $x = 0.05$ (a), 0.075 (b), and 0.1 (c). Inset to (b) shows variation in peak resistivity temperature T_P with composition and magnetic field.

approximately equal ionic size of the dopants negate the effects of lattice strain in these compounds. The results are very systematic in terms of the decrease in resistivity of the Ho compositions in comparison to that of the Y compositions as well as in terms of the shift in T_C/T_P to low temperatures with increase in doping level. These results cannot be attributed to the effects such as oxygen stoichiometry as well as grain boundaries that have been assumed to be the same, keeping in mind the identical conditions under which the compounds were prepared. The microstructure of the compounds were compared using a scanning electron microscope. All the compounds were found to have a similar microstructure. Microstructural effects that purely depend on the annealing conditions cannot give rise to such systematic differences in resistivity between the Ho- and Y-doped compounds. The weight difference between the substituted ions (Ho and Y in this case) also does not play any role in the observed properties of the compounds. This is because weight differences between substituted ions are usually seen to effect the Curie temperature as reported by oxygen-isotope experiments.[23] In this case since the mass of the Ho ion is greater than that of the Y ion, T_C/T_P of Ho-doped compounds of the same concentration should have been greater than that of the Y-doped compounds (since greater mass ensures greater electron-phonon coupling and hence lower T_C/T_P). However, such differences in T_C/T_P for the same concentration of Ho- and Y-doped compounds were not observed. Thus the observed differences in the resistivity cannot be attributed to microstructural effects or to the weight differences between the substituted ions.

Figure 2(a) shows the temperature dependence of resistivity for the $x = 0.05$ composition of both Ho- and Y-doped LCMO at magnetic fields of 0, 4, and 8 T. It can be clearly noticed that the peak resistivity temperature T_P at zero field is nearly the same in both the cases (Ho and Y) indicating that the shift in T_P from that of pure LCMO ($T_P = 260$ K) is the same because of the identical ionic radii of Ho and Y.[24] As there are substantial differences in the magnetic moments of the substituted ions, the decrease in resistivity of the Ho-doped compound could be attributed to the magnetic moment ($10.4\mu_B$) of the Ho ion.

Figures 2(b) and 2(c) show $\rho - T$ behavior for the $x = 0.075$ and 0.1 compositions. Inset to Fig. 2(c) shows the

same for the Y(0.1) composition. It is seen from inset to Fig. 2(b) that in general, the supression in T_P is greater for the Y compounds compared to the Ho compounds. The difference in T_P increases with increase in magnetic field for the $x=0.05$ and 0.075 compositions whereas it decreases for the 0.1 composition. This shows that the presence of a magnetic field increases the ferromagnetic coupling for the $x=0.05$ and 0.075 compositions whereas for the $x=0.1$ composition, the decrease in the difference in T_P with increase in magnetic field could be attributed to the presence of competing ferromagnetic and antiferromagnetic interactions that tend to give rise to a magnetic frustration thus reducing the ferromagnetic coupling as will be confirmed later. It must be noted here that the effect of smaller (compared to average *A*-site ionic radius in pure LCMO) *A*-site ionic size in decreasing the ferromagnetic coupling by reducing the overlap between the Mn 3*d* orbitals is the same. Thus the observed differences in the resistivity of the Ho and Y compounds could be attributed to the increase in the net magnetic moment of the Mn ion in the Ho compounds and hence an increase in the ferromagnetic coupling between adjacent Mn ions. The increase in the net magnetic moment has been further confirmed by magnetization measurements.

Figure 3 shows magnetization of the compounds as a function of temperature at fields of 0.1 T and 14 T. A comparison of these curves at the two fields shows the absence of a clear transition temperature at higher fields. This is because of the presence of magnetic inhomogeneities that order over a wide range of temperature. Also the fact that above 40 K the magnetizations M of the Ho-doped compounds are such that $M(\mathrm{Ho}_{0.05})<M(\mathrm{Ho}_{0.075})<M(\mathrm{Ho}_{0.1})$ is because $T_C(\mathrm{Ho}_{0.05})<T_C(\mathrm{Ho}_{0.075})<T_C(\mathrm{Ho}_{0.1})$. Since magnetization at any temperature is proportional to the number of ordered moments at that temperature, at any temperature above 40 K there will be more number of ordered moments in a compound that has lower T_C, unless the temperatures are so high enough so that there is same amount of spin disorder in all the compounds. For the $x=0.05$ composition, there is a very small increase in the magnetization of the Ho compound in comparison to that of the Y compound at low fields and low temperatures. However for higher compositions the significant difference between the magnetization values of the Ho and Y compounds clearly shows a net ferromagnetic coupling of the Mn moment with that of the rare-earth moment. The fact that even at high magnetic fields (14 T) the full expected saturation magnetization value is reached only well below T_C is because of the lack of a long-range cooperative ordering phenomena unlike in classical ferromagnets. The saturation magnetization for $x=0.05$ and 0.075 of the Y compounds is about $3.8\mu_B$ per Mn ion, which is close to the expected spin-only moment of Mn. However, for the same field and for the same compositions of the Ho-doped samples the values are $4.3\mu_B$ and $4.4\mu_B$, respectively. The spin-only moment of Mn ion in these compounds[10,15] is $0.7(4\mu_B)+0.3(3\mu_B)=3.7\mu_B$. If we assume a coupling of the Ho moment with that of the Mn moment in the case of the Ho compositions, then for the 0.05 composition, the net magnetic moment per Mn ion should be $0.05(10.4\mu_B)+3.7\mu_B=4.22\mu_B$ while for the 0.075 composition the net magnetic moment should be $0.075(10.4\mu_B)+3.7\mu_B=4.48\mu_B$. These are approximately the values of the magnetic moments obtained from our magnetization data (Fig. 3), thus confirming our hypothesis. This result is remarkable since it provides evidence for coupling of the magnetic moments of the Ho ions with that of the Mn ions in the lattice. The increase in the net magnetic moment of the Mn ion should increase the ferromagnetic coupling between adjacent Mn ions and thereby the effective electronic bandwidth. This explains the decrease in the resistivity of the Ho compositions. The increase in the net magnetic moment of the Mn-ion can also be explained in terms of the aspherical screening of the rare-earth (Ho) valence shell.[14] This aspherical property produces a local lattice distortion around the Ho ion that favors a ferromagnetic coupling between adjacent Mn ions thus giving rise to a local ferromagnetic cluster. Furthermore, from the M versus H curves it is evident that at $T=4.2$ K for the

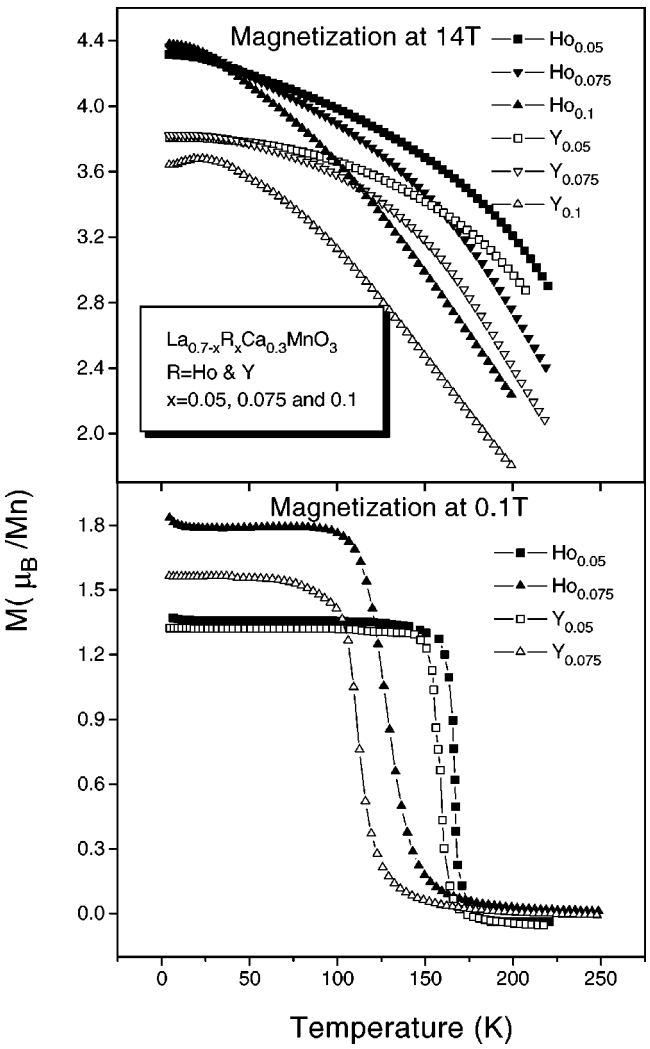

FIG. 3. Magnetization versus temperature for $(\mathrm{La}_{0.7-x}R_x)\mathrm{Ca}_{0.3}\mathrm{MnO}_3$ ($R=$Ho, Y) with $x=0.05$, 0.075, and 0.1 at magnetic fields of 14 T and 0.1 T showing increase in saturation magnetization for the Ho-doped compounds at low temperatures. It is seen that the magnetic moment per Mn ion for the Ho compounds is greater than the free-ion moment indicating a coupling of the Ho moment to the Mn moment.

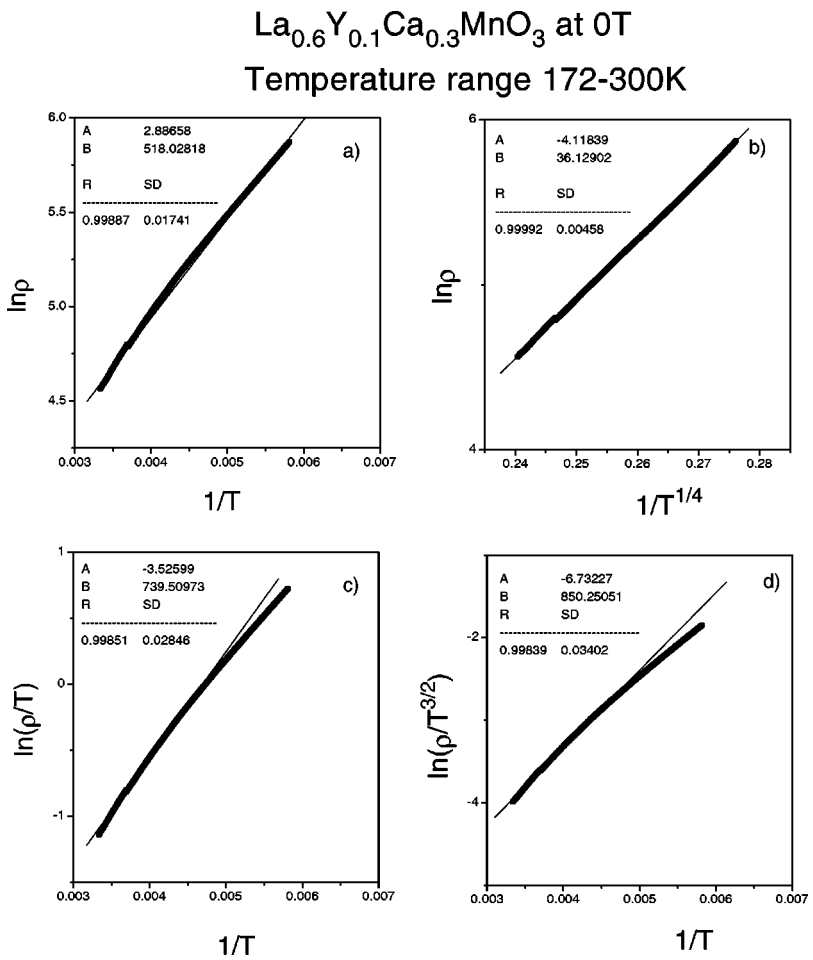

FIG. 4. (a) $\ln\rho$ versus $1/T$, (b) $\ln\rho$ versus $1/T^{1/4}$, (c) $\ln(\rho/T)$ versus $1/T$, and (d) $\ln(\rho/T^{3/2})$ versus $1/T$ plots for $La_{0.6}Y_{0.1}Ca_{0.3}MnO_3$ indicating fits of the resistivity data to Arrhenius, 3D VRH, adiabatic polaron, and nonadiabatic polaron models. The linear correlation coefficient R shown in the figure quantitatively gives the quality of the fit. A and B values given in each of the figures stand for the intercept and slope, respectively.

Ho-doped samples in our experiments the saturation magnetization is already reached in a field of 14 T. This is in contrast to the Dy-doped samples, where saturation was obtained only at about 50 T.[15]

In order to understand the transport mechanism in these compounds, the resistivity data was analyzed separately in the two regimes (metallic and insulating). The resistivity data in the insulating regime were fitted to the variable range hopping (VRH) and the polaron models. There have been several contradicting reports about the validity of VRH (Refs. 10–16 and 24) or polaronic models[18–20,25] in manganites. Our fits unequivocally show that Mott's VRH mechanism[26] is the prevalent mechanism in these compounds and our results corroborate with other groups.[10] The resistivity data above T_P in all cases fitted well to an equation of the form

$$\rho = \rho_\infty \exp(T_0/T)^{1/4}, \tag{1}$$

which represents a three-dimensional 3D VRH mechanism and the localization lengths in each case were evaluated using the expression

$$k_B T_0 = 18\alpha^3/3N(E_F), \tag{2}$$

where α is the inverse localization length and $N(E_F)$ is the density of states at the Fermi energy.

A comparison between the 3D-VRH fits and the polaron fits is shown in Fig. 4. The nature of the fit was ascertained from R (linear correlation coefficient) and the standard deviation values in each case. It was found that when a constant value of $N(E_F)=4\times10^{28}/\mathrm{eV\,m^3}$ $[\mathrm{N}(E_F)1]$ was assumed,[10,11] the values of localization length obtained were unrealistically small (<1 Å). It was suggested by Viret *et al.*[10] that the origin of these unphysically small values of a and R is the presence of a magnetic-localization mechanism over and above the Anderson localization. Apart from the random potential fluctuations in the Coulomb potential due to the A^{3+} and B^{2+} ions, the e_g electrons could further be trapped by fluctuations in the spin-dependant potential due to local deviations from ferromagnetic order. Based on these considerations, they found an effective density of states of the order of $N_{eff}=9\times10^{26}/\mathrm{eV\,m^3}$. The localization lengths evaluated using this value of $N(E_F)$ are shown in Table I and the values are very reasonable. The value of localization length obtained on one of our compounds ($La_{0.6}Y_{0.1}Ca_{0.3}MnO_3$) is in excellent agreement with the value obtained by Sergeenkov *et al.*[27]

TABLE I. Localization lengths calculated using variable range hopping (VRH) and magnetic localization (ML) models at different magnetic fields for $La_{1-x}R_xMnO_3$ (R=Ho, Y and x=0.05, 0.075, and 0.1) compounds.

Composition	Applied field (T)	T_0 (K)		Localization length Å		
		VRH[a]	ML[b]	$N(E_F)1$[c]	$N(E_F)2$[d]	ML
Ho(0.05)	0	9.18×10^7		0.369	1.337	
Ho(0.05)	4	3.51×10^7	3.05×10^7	0.509	1.9	1.947
Ho(0.05)	8	5.49×10^6	8.66×10^6	0.945	3.016	2.964
Ho(0.075)	0	1.06×10^8		0.352	1.437	
Ho(0.075)	4	6.3×10^7	6.97×10^7	0.419	1.602	1.479
Ho(0.075)	8	3.38×10^7	3.67×10^7	0.515	1.953	1.831
Ho(0.1)	0	1.62×10^8		0.305	1.032	
Ho(0.1)	4	6.73×10^7	4.27×10^7	0.409	1.802	1.741
Ho(0.1)	8	3.19×10^7	1.82×10^7	0.525	2.239	2.311
Y(0.05)	0	1.2×10^8		0.337	1.239	
Y(0.05)	4	6.89×10^7	6.55×10^7	0.406	1.54	1.51
Y(0.05)	8	2.68×10^7	2.53×10^7	0.557	2.133	2.073
Y(0.075)	0	1.14×10^8		0.343	1.322	
Y(0.075)	4	7.67×10^7	5.46×10^7	0.392	1.464	1.604
Y(0.075)	8	3.59×10^7	2.56×10^7	0.505	1.939	2.064
Y(0.1)	0	1.2×10^8		1.396	5.167	
Y(0.1)	4	8.95×10^5	9.49×10^5	1.73	6.405	6.194
Y(0.1)	8	8.73×10^5	8.33×10^5	1.744	6.482	6.465

[a]Variable-range-hopping model.
[b]Magnetic-localization model.
[c]4×10^{22}/eV cm^3.
[d]9×10^{26}/eV cm^3.

TABLE II. Comparison of residual-resistivity values obtained experimentally as well as from the theoretical fits. Also seen is a comparison of the residual resistivity values for the same compound at different magnetic fields and a comparison between similar compositions of Ho and Y at the same field.

Composition	Applied field (T)	ρ_0 (mΩ cm)	ρ_0 (mΩ cm) values obtained from theoretical fit	% change with respect to 0 T	% change with respect to Ho at the same field of Y
Ho(0.05)	0	33.0	36.2		
Ho(0.05)	4	11.2	16.5	66.1	
Ho(0.05)	8	10.0	7.8	70.5	
Ho(0.075)	0	67.4	54.3		
Ho(0.075)	4	41.0	33.0	90.1	
Ho(0.075)	8	20.0		95.2	
Ho(0.1)	0	1510			
Ho(0.1)	4	319	414	78.8	
Ho(0.1)	8	222	243	85.3	
Y(0.05)	0	75.7	92.2		94.6
Y(0.05)	4	51.0	55.9	34.6	97.2
Y(0.05)	8	21.0	24.2	96.6	53.1
Y(0.075)	0	861	1089		52.0
Y(0.075)	4	102	248	88.1	60.3
Y(0.075)	8	63.4	126	92.6	68.7
Y(0.1)	0	324018	380111		99.5
Y(0.1)	4	125528	129849	61.2	99.7
Y(0.1)	8	95558	96987	70.5	99.7

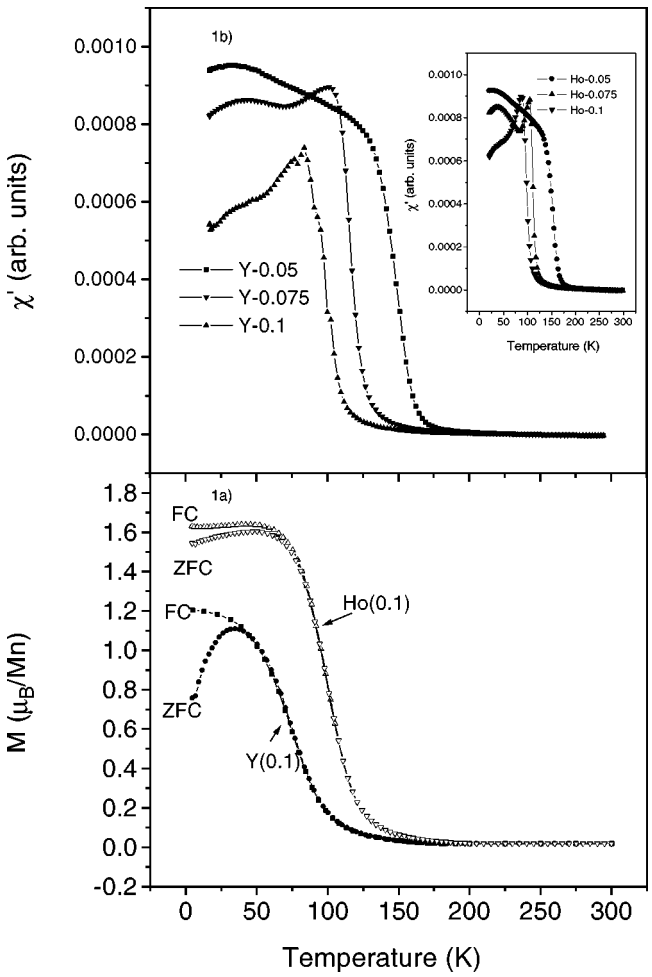

FIG. 5. (a) Deviation in field-cooled (FC) and zero-field-cooled (ZFC) magnetization curves at 0.1 T seen in the case of $x=0.1$ compositions of Ho- and Y-doped compounds. The deviation is greater for the Y-doped compounds indicating spin-glass-like behavior. (b) ac-susceptibility curves confirming the above observation.

It is seen from Table I that, in general, the localization length values are greater for the Ho compounds compared to the Y compounds. However for the 0.1 compositions there is a sudden jump in the values for the Y compounds that has been attributed to a spin-glass-like nature, confirmed by field-cooled (FC) and zero-field-cooled (ZFC) measurements as shown in Fig. 5.

This is the reason why the systematic increase of saturation magnetization M_s values obtained in the case of 0.05 and 0.075 Ho doping is not seen in the case of the 0.1-dopant composition of Ho and Y compounds.

In the presence of an applied magnetic field Viret *et al.*[10] found the resisitivity to follow an equation of the type

$$\rho=\rho_\infty \exp\{T_0[1-(M/M_s)^2]/T\}^{1/4}, \tag{3}$$

where $M=M_s\cos\theta_{ij}$ is the local magnetization and M_s is the saturation magnetization.

The resistivity data above T_P for magnetic fields of 4 and 8 T were fitted to the above equation using M/M_S values that

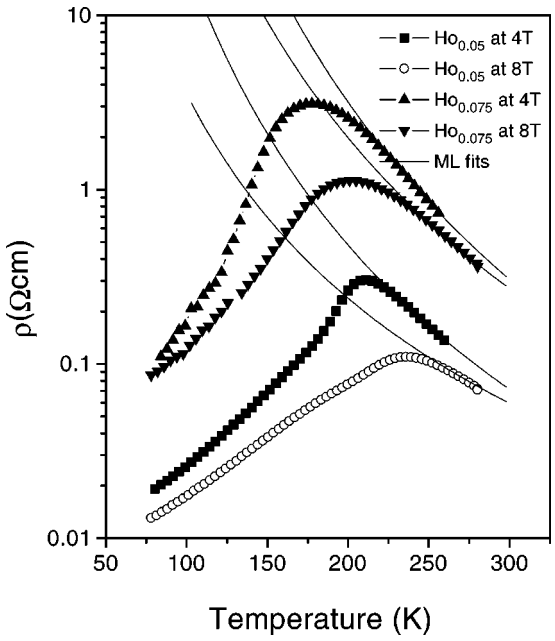

FIG. 6. Magnetic-localization model fits of the resistivity data for the $x=0.05$ and 0.075 compositions.

were obtained from the Brillouin function for the respective magnetic fields taking $J=S=3/2$ (Mn^{4+}) and the localization lengths were again calculated as shown in Table I. It is seen that the values of localization length obtained using the new value of $N(E_F)$ and the magnetic-localization model are in excellent agreement. This clearly shows that above T_P the electronic states are localized by a random potential, which is mainly magnetic in origin and conduction is by a 3D-VRH mechanism between these states. The theoretical fits of the resistivity data above T_P to the magnetic localization model is shown in Fig. 6.

In general, the resistivity data in the metallic regime was found to fit to an equation of the form[28]

$$\rho=\rho_0+\rho_1T^2+\rho_2T^{4.5}, \tag{4}$$

which indicates a combination of electron-electron, electron-phonon and electron-magnon scattering. Table II shows a comparison of the residual resistivity values obtained from the experimental curves and the theoretical fits. The values obtained from the theoretical fits are in excellent agreement with those obtained from the experimental curves. It is seen here that, in general, the values decrease with increase in field for the same composition indicating the presence of lattice imperfections that are magnetically coupled. However, the huge percentage changes in the values of the Y compositions with respect to the Ho compositions at the same field indicates the relative amount of order that is brought about in the Ho compositions by the coupling of the Ho moment with that of the Mn moment in the lattice. Figure 2(c) shows clearly the large difference in the residual resistivity values that is seen in the case of the 0.1 composition. From these values, the canting angles at the boundaries of the wave packet were calculated[29] using the equation

$$\rho_0 = \rho_m \exp[2U_H(1-\cos\phi)/k\theta_D], \quad (5)$$

where ρ_m is a typical metallic resistivity (1.5×10^{-6} Ω m), $U_H = 2$ eV, θ_D is the Debye temperature, and ϕ is the canting angle between adjacent wave packets that characterize a large magnetic spin polaron. It was seen here that the canting-angle values were in general small for the Ho compounds compared to the Y compounds [e.g., it is 24.5° for Ho(0.1) at 0 T and 29.3° for Y(0.1) at 0 T] indicating less spin disorder and less resistivity in the former. This result will be reported elsewhere.

Our systematic studies to find the effect of doping Ho (magnetic) at the La site in LCMO compared to Y (nonmagnetic) showed dramatic results. Ho-doped compounds show less resistivity compared to Y-doped compounds and yield large values of localization length compared to the latter. Magnetization measurements confirm an increase in the effective magnetic moment of Mn ion in the case of $x = 0.05$ and 0.075 compositions of the Ho-doped compounds thus showing a coupling of the Ho moments with those of the Mn moments in the lattice. Spin-glass-like behavior was obtained in the case of 0.1 (Ho/Y) compositions. Residual resistivity values show the presence of lattice imperfections that are magnetically coupled.

M.S.R.R. would like to thank the AvH Foundation for financial support.

*Corresponding author; email address: msrrao@iitm.ac.in

[1] G.H. Jonker and J.H. Van Santen, Physica (Amsterdam) **16**, 337 (1950).
[2] E.O. Wollan and W.C. Koehler, Phys. Rev. **100**, 548 (1955).
[3] R.M. Kusters, J. Singleton, O.A. Keen, R. McGreevy, and W. Hates, Physica B **155**, 362 (1989).
[4] R. Von Helmholt, J. Werker, B. Holzapfeil, L. Schultz, and K. Samwer, Phys. Rev. Lett. **71**, 2331 (1993).
[5] S. Jin, T.H. Tiefel, M. McCormack, R.A. Fastnacht, R. Ramesh, and L. Chen, Science **264**, 413 (1994).
[6] C. Zener, Phys. Rev. **82**, 403 (1951).
[7] P.G. de Gennes, Phys. Rev. **118**, 141 (1960).
[8] K. Kubo and N. Ohata, J. Phys. Soc. Jpn. **33**, 21 (1972).
[9] A.J. Millis, P.B. Littlewood, and B.I. Shraiman, Phys. Rev. Lett. **74**, 5144 (1995).
[10] M. Viret, L. Ranno, and J.M.D. Coey, Phys. Rev. B **55**, 8067 (1997); Phys. Rev. Lett. **75**, 3910 (1995).
[11] J.M.D. Coey, M. Viret, and S. von Molnar, Adv. Phys. **48**, 167 (1999).
[12] Masatoshi Imada, Atsushi Fujimori, and Yoshinori Tokura, Rev. Mod. Phys. **70**, 1039 (1998).
[13] P.A. Lee and T.V. Ramakrishnan, Rev. Mod. Phys. **57**, 287 (1985).
[14] K. Nicholson, U. Häfner, E. Müller-Hartmann, and D. Wohlleben, Phys. Rev. Lett. **41**, 1325 (1978).
[15] T. Terai, T. Kakeshita, T. Fukuda, T. Saburi, N. Takamoto, K. Kindo, and M. Honda, Phys. Rev. B **58**, 14 908 (1998).
[16] P. Wagner, V. Metlushko, L. Trappeneirs, A. Vantomme, J. Vanacken, G. Kido, V.V. Moshchalkov, and Y. Bruynseraede, Phys. Rev. B **55**, 3699 (1997); see also P. Wagner, I. Gordon, L. Trappeniers, J. Vanacken, F. Herlach, V.V. Moschalkev, and Y. Bruynseraede, Phys. Rev. Lett. **81**, 3980 (1998).
[17] G. Schnyder, R. Hiskes, S. DiCarolis, M.R. Beasley, and T.H. Geballe, Phys. Rev. B **53**, 1 (1996).
[18] M. Jaime, H.T. Hardner, M.B. Salamon, M. Rubinstein, P. Dorsey, and D. Emin, Phys. Rev. Lett. **78**, 951 (1997).
[19] D.C. Worledge, L. Mieville, and T.H. Geballe, J. Appl. Phys. **83**, 5913 (1998).
[20] J.M. De Teresa, M.R. Ibarra, P.A. Algarabel, C. Ritter, C. Marquina, J. Blasco, J. Garcia, A. del Moral, and Z. Arnold, Nature (London) **386**, 256 (1997).
[21] C.H. Booth, F. Bridges, G.J. Snyder, and T.H. Geballe, Phys. Rev. B **54**, R15 606 (1996).
[22] H.Y. Hwang, S.W. Cheong, P.G. Radaelli, M. Marezio, and B. Batlogg, Phys. Rev. Lett. **75**, 914 (1995).
[23] Guo-meng Zhao, K. Conder, H. Keller, and K.A. Muller, Nature (London) **381**, 676 (1996).
[24] P. Wagner, I. Gordon, A. Vantomme, D. Dierickx, M.J. Van Bael, V.V. Moshchalkov, and Y. Bruynseraede, Europhys. Lett. **41**, 49 (1998).
[25] H. Roder, J. Zhang, and A.R. Bishop, Phys. Rev. Lett. **76**, 1356 (1996).
[26] N.F. Mott, *Metal-Insulator Transitions* (Taylor & Francis, London, 1990).
[27] S. Sergeenkov, H. Bougrine, M. Ausloos, and A. Gilbert, Phys. Rev. B **60**, 12 322 (1999).
[28] V. Ravindranath, M.S. Ramachandra Rao, and G. Rangarajan (unpublished).
[29] V. Ravindranath, M.S. Ramachandra Rao, and R. Gross (unpublished).